Polarized Skylight Navigation in Insects: Model and Electrophysiology of e-Vector Coding by Neurons in the Central Complex

Midori Sakura, Dimitrios Lambrinos and Thomas Labhart

J Neurophysiol 99:667-682, 2008. First published 5 December 2007; doi:10.1152/jn.00784.2007

J Neurophysiol 99: 667–682, 2008.
First published December 5, 2007; doi:10.1152/jn.00784.2007.

Polarized Skylight Navigation in Insects: Model and Electrophysiology of e-Vector Coding by Neurons in the Central Complex

Midori Sakura, Dimitrios Lambrinos, and Thomas Labhart
Institute of Zoology, University of Zurich, Zurich, Switzerland

Submitted 12 July 2007; accepted in final form 5 December 2007

Sakura M, Lambrinos D, Labhart T. Polarized skylight navigation in insects: model and electrophysiology of e-vector coding by neurons in the central complex. *J Neurophysiol* 99: 667–682, 2008. First published December 5, 2007; doi:10.1152/jn.00784.2007. Many insects exploit skylight polarization for visual compass orientation or course control. As found in crickets, the peripheral visual system (optic lobe) contains three types of polarization-sensitive neurons (POL neurons), which are tuned to different (~60° diverging) e-vector orientations. Thus each e-vector orientation elicits a specific combination of activities among the POL neurons coding any e-vector orientation by just three neural signals. In this study, we hypothesize that in the presumed orientation center of the brain (central complex) e-vector orientation is population-coded by a set of "compass neurons." Using computer modeling, we present a neural network model transforming the signal triplet provided by the POL neurons to compass neuron activities coding e-vector orientation by a population code. Using intracellular electrophysiology and cell marking, we present evidence that neurons with the response profile of the presumed compass neurons do indeed exist in the insect brain: each of these compass neuron-like (CNL) cells is activated by a specific e-vector orientation only and otherwise remains silent. Morphologically, CNL cells are tangential neurons extending from the lateral accessory lobe to the lower division of the central body. Surpassing the modeled compass neurons in performance, CNL cells are insensitive to the degree of polarization of the stimulus between 99% and at least down to 18% polarization and thus largely disregard variations of skylight polarization due to changing solar elevations or atmospheric conditions. This suggests that the polarization vision system includes a gain control circuit keeping the output activity at a constant level.

INTRODUCTION

As a result of sunlight scattering in the atmosphere, skylight is partially plane-polarized, i.e., in any point of the sky a particular orientation of the electric vector (e-vector) of light dominates (Strutt 1871; for graphical representations of the celestial polarization pattern, see Fig. 1 in Wehner 1997). Many insects exploit skylight polarization for visual compass orientation. Crickets have been proposed to observe the average e-vector orientation in their upper visual field for this task (Labhart and Meyer 2002; Wehner and Labhart 2006). As in other insects (for a review, see Labhart and Meyer 1999), the detection of polarized skylight in crickets is mediated by specialized, strongly polarization-sensitive photoreceptors situated at the dorsal rim of the compound eye, termed dorsal rim area (DRA) (Blum and Labhart 2000; Brunner and Labhart 1987; Burghause 1979).

As shown in crickets and ants, e-vector information collected by the photoreceptors of the DRA is processed by polarization-sensitive neurons in the optic lobe (POL neurons) (Labhart 1988, 2000), the best studied of which are the POL1 neurons of crickets (Labhart 1996, 1999; Labhart et al. 2001; Petzold 2001). In these neurons, spiking activity is a sinusoidal function of e-vector orientation with alternating parts of excitation and inhibition and with the maxima and minima 90° apart. Their wide visual fields (>60°) are directed to the upper part of the sky. POL1 neurons have important signal conditioning functions: The polarization-antagonism generates a differential signal, which effectively enhances polarization contrast and removes information on light intensity. In addition, spatial integration increases absolute sensitivity and makes the system insensitive to disturbances in the polarization pattern such as those caused by clouds (Labhart 1999; Labhart et al. 2001). Thus POL1 neurons remove irrelevant and unreliable features from the celestial stimulus, conditioning the polarization signal for further processing.

There are three types of POL1 neuron tuned to different e-vectors oriented ~10, 60, and 130° to the long axis of the head. The POL1 neurons seem to represent the first processing layer of an "instantaneous" system of polarization vision, in which e-vector orientation is unambiguously defined by the signals of three differently-tuned, polarization-sensitive input channels (triplet code) (Bernard and Wehner 1977; Lambrinos et al. 1997, 2000). This is reminiscent of a trichromatic color vision system, in which color is coded by the signals of three spectral types of photoreceptor. To read the triplet code of e-vector orientation, the signals of the three POL1 neurons must be compared in some way. Two different mathematical decoding algorithms have been proposed. They were successfully tested in mobile robots, which were equipped with optoelectronic polarization sensors mimicking insect POL neurons (Lambrinos et al. 1997, 2000). However, these algorithms did not take in account the constraints of actual neural circuits. For instance, they contained complex mathematical operations, such as trigonometric functions without proposing any neural implementations (Lambrinos et al. 1997, 2000). Moreover, the output of these procedures is incompatible with the observed map-like representation of visual features in the brain (e.g., edge orientation: Bonhoeffer and Grinwald 1993; Hubel and Wiesel 1968; movement direction: Wellky et al. 1996; spatial frequency: Tootell et al. 1988; color: Ts'o and Gilbert 1988; Xiao et al. 2003).

Address for reprint requests and other correspondence: T. Labhart, Institute of Zoology, University of Zurich, Winterthurerstr. 190, CH 8057 Zurich, Switzerland (E-mail: labhart@zool.uzh.ch).

The costs of publication of this article were defrayed in part by the payment of page charges. The article must therefore be hereby marked "*advertisement*" in accordance with 18 U.S.C. Section 1734 solely to indicate this fact.

Our study employs two approaches. Using *computer modeling*, we designed an artificial neural network, which transforms the signal triplet of the modeled POL neurons to activities of a set of 12 "compass neurons" providing a map-like representation of e-vector orientation (population code). Thus the triplet code consisting of three activity values is mapped to a larger population code of 12 signals. The neural network is based on an algorithm that differs from the previously used mathematical solutions (Lambrinos et al. 1997, 2000) in the following way. *1*) It uses only simple mathematical operations, i.e., addition and subtraction, simulating synaptic excitation and inhibition, respectively, and a threshold function. *2*) It is a parsimonious solution, which can readily be represented by a simple neural network. And *3*) the output is compatible with a map-like representation of e-vector orientation in the brain. However, by adding and subtracting spike frequencies, the synaptic connections of the network are coarse imitations of real synapses, which are acceptable under certain constraints only (for details, see DISCUSSION). Although this model remains a strong simplification of any biological neural circuit, it proved useful for studying the flow of sensory information in coding e-vector orientation. We will refer to it as "neural network model" or "network model" to distinguish it from the algorithms previously employed in navigating robots (Lambrinos et al. 1997, 2000). We demonstrate that the network model extracts e-vector orientation from the three POL neuron signals with the same high precision as the previously proposed algorithms.

Using *intracellular electrophysiology*, we recorded from polarization-sensitive neurons in the central complex of the cricket brain. We demonstrate that neurons with the response profile of compass neurons, as proposed by the network model, do indeed exist in the insect brain: they are activated by certain e-vector orientations and otherwise remain silent. These neurons are strongly reminiscent of the "head direction" cells recorded in the vertebrate brain, neurons that are active only when the head points in a certain direction with respect to the visual environment, thus signaling to the animal the direction in which it is oriented (e.g., Taube 1998; Taube et al. 1990). Surpassing the modeled compass neurons in performance, the polarization-sensitive neurons in the insect central complex are insensitive to the degree of polarization over a large range, suggesting that the polarization vision system includes a gain control circuit. Thus under natural conditions, they disregard variations of the degree of polarization in the sky caused by changing solar elevations or atmospheric conditions.

METHODS

Computer modeling

NEURAL NETWORK MODEL: ORIGINAL VERSION. The neural network model is a hypothesis of how the insect brain processes the sensory signals of polarization-sensitive input neurons to form a map-like neural representation of e-vector orientation in the brain. In particular, it transforms the triplet code for e-vector orientation provided by POL neurons in the optic lobe to a population code expressed by a number of compass neurons in the brain. The neural network consists of three layers of neurons interconnected in a feed-forward manner (Fig. 1*A*). Note that in the graphical representation of the network, individual afferent neurons can make both excitatory and inhibitory connections. For clarity, we do without drawing polarity-switching intervening neurons in the inhibitory pathways.

The *first layer* contains three neurons (1st-order neurons or POL neurons in Fig. 1*A*) providing input to the system. They represent neurons responding in an analogous way as cricket POL1 neurons or pooling neurons receiving bilateral input from such neurons without any preprocessing. The activities of the model POL neurons are sinusoidal functions (log $\cos^2$ functions) of e-vector orientation with a period of 180°, exhibiting maximum spike activities at the tuning e-vector orientations φ_{max} of 0, 60, and 120° (relative to the long axis of the head). The response functions of the first-order neurons are shown in Fig. 1*B* (*top graph*). For a formal description of the response functions see APPENDIX, *Eq. A1*.

The *second layer* consists of six neurons (2nd-order neurons in Fig. 1*A*). Every second-order neuron receives input from two first-order neurons through excitatory and inhibitory afferent connections. The result of these operations is a new set of six neurons with sinusoidal response functions and six different e-vector tuning axes φ_{max}, namely at 15, 45, 75, 105, 135, and 165°, relative to the long axis of the head. The response functions (in spike/s) of the second-order neurons are shown in Fig. 1*B* (*middle graph*). For a formal description of the response functions, see APPENDIX, *Eqs. A2* and *A3*.

The *third layer* consists of 12 neurons (3rd-order neurons or compass neurons in Fig. 1*A*) and receives input from the second-order neurons. The third-order neurons have their e-vector tuning axes φ_{max} at 0, 15, 30, . . . , 180° with 15° increments, relative to the long axis of the head. To reduce spiking activity of the third-order neurons to e-vector ranges of 90°, a spiking threshold corresponding to 55 spikes/s is applied. The response functions (in spikes/s) of the third-order neurons are shown in Fig. 1*B* (*bottom graph*). For a formal description of the response functions, see APPENDIX, *Eqs. A4–A6*. By entering the activity levels of the 12 compass neurons into a bar graph, activity patterns of compass neurons for any e-vector orientation are obtained (indicated for three e-vector orientations in Fig. 1*C*).

NEURAL NETWORK MODEL: EXTENDED VERSION. In the original neural network, the output activity of the compass neurons is a function of the degree of polarization *d*. To adapt the model to the experimental data obtained from compass-neuron like cells, which exhibit independence of *d*, an additional (4th) layer containing 12 neurons was added (Fig. 1*D*). These neurons represent the compass neurons of the extended network. Each of these neurons is connected to a single neuron in the third layer through one excitatory afferent and one excitatory efferent connection, creating a positive feedback loop (a self-exciting loop) and thus amplifying the signals of the fourth layer neurons (e.g., Douglas et al. 1995). All neurons of the fourth layer send their output to a single interneuron, the gain control neuron (GCN). Its role is to control the activity in the fourth layer and prevent runaway excitation. The GCN, which receives excitatory input from all neurons in the fourth layer, sends its output to all the third-order neurons through inhibitory efferent connections. The GCN is active only when the sum of its inputs (from the 4th-order neurons) exceeds a certain threshold. Thus the GCN suppresses the feedback loop once the activity of the fourth-order neurons reaches a certain level, keeping their activity at a constant level. For a formal description of the gain control circuit, see APPENDIX, *Eqs. A7–A10*.

BENCHMARKING THE POPULATION CODE. The activation pattern of the compass neurons (Fig. 1*C*) represents the output of the polarization compass, providing the insect with a map-like representation of e-vector orientation (population code). To assess the precision of that map, we calculated the weighted average of compass neuron activity (population median, also called population vector).

Individual compass neurons represent discrete e-vector orientations. They make contributions to overall compass neuron activity

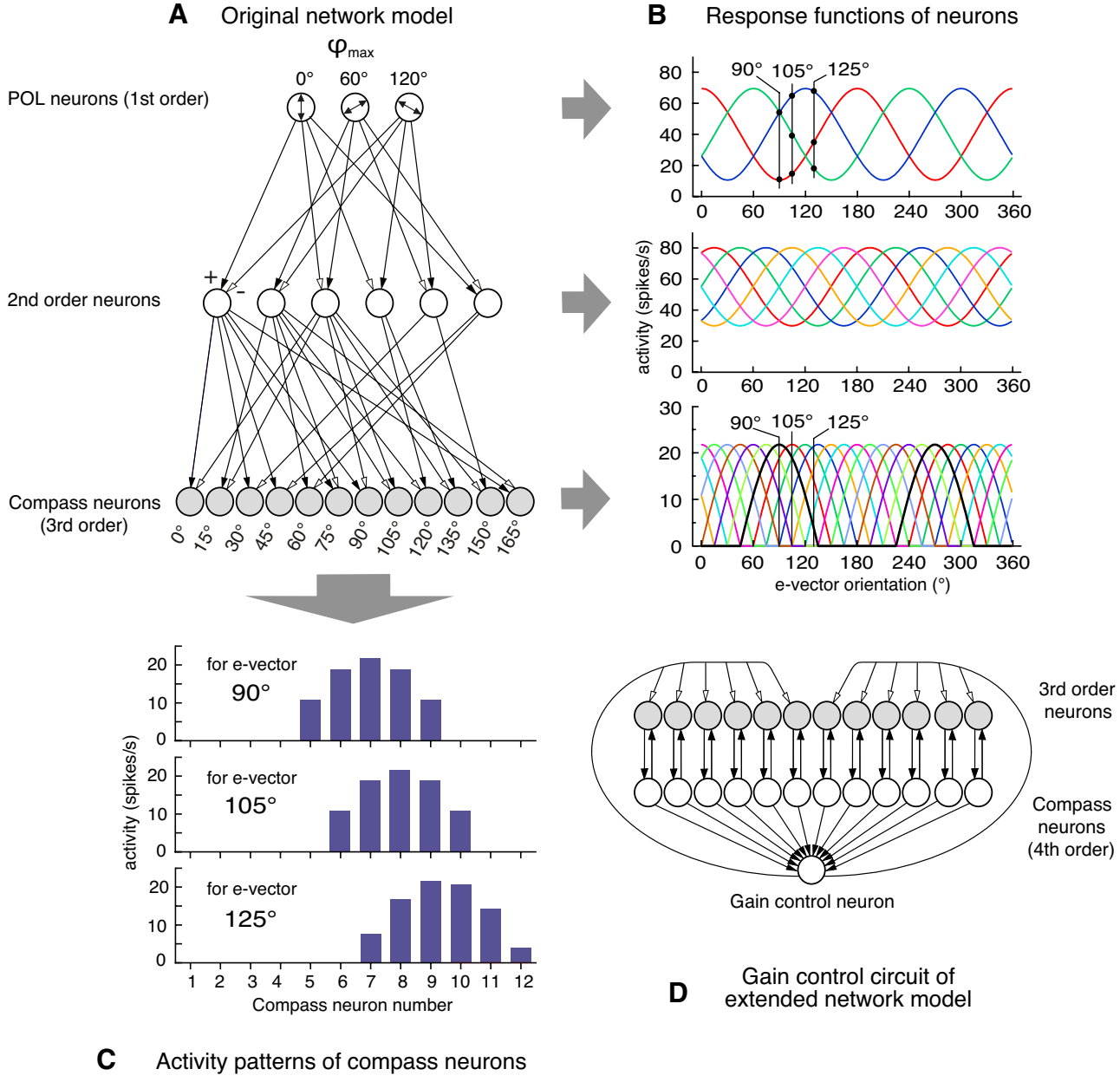

FIG. 1. Artificial neural network converting the signals of three input neurons tuned to e-vector orientations of 0, 60, and 120° to activity patterns of output neurons. The network converts the triplet code of e-vector orientation to a population code. *A*: architecture of the original neural network model. The activity of the input neurons (POL neurons) is propagated through layers of neurons in a feed-forward antagonistic way. To the 3rd layer (compass neurons), a threshold function is applied. Black arrowheads, excitation; white arrowheads, inhibition. Degree values next to POL neurons and compass neurons indicate e-vector orientations to which neurons are tuned. *B*: e-vector response functions for POL neurons, 2nd-order neurons and compass neurons (*top* to *bottom graph*). POL neuron response functions are modeled log $\cos^2$ functions. Triplet values provided by the POL neurons at 90, 105, and 125° e-vectors (*top graph*) correspond to activities of compass neurons at these orientations (*bottom graph*). *C*: activity patterns of compass neurons for 90, 105, and 125° e-vector orientations (*top* to *bottom graph*) as read from *bottom graph* in *B*. Degree of polarization $d = 0.4$ in *B* and *C*. *D*: architecture of the gain control mechanism of the extended neural network model. The 3rd-order neurons of the original network (gray neurons in *A* and *D*) have additional connections with a 4th layer of neurons (compass neurons) and a gain control neuron implementing a gain control circuit. The connections between 2nd- and 3rd-order neurons are as in the original network (*A*). Arrowheads are as in *A*.

in proportion to their respective activity. The population median is the center of gravity of the active population of compass neurons (for a formal description of the population median, see APPENDIX, *Eq. A11*). Because the activity level of each neuron is a real number (continuous quantity), the population median will also be a real number despite the fact that the neuron indices are integers. Thus the population median is a continuous representation of the e-vector orientation. Because the median is a real number it can be converted to degrees by mapping its range from [1,12] to [0°,180°].

Electrophysiological experiments

ANIMAL PREPARATION AND RECORDING. Adult black crickets, *Gryllus bimaculatus*, were used for the experiments. They were either from an old laboratory stock (originating from Cyprus) or from a new stock founded in 2004 with animals from Tunisia. The crickets were kept and bred under long-day conditions (14 h L:10 h D) at 26°C and 60% relative humidity. Lighting was provided by Osram L20W/10S daylight lamps. Crickets were waxed to a stage, and a small window

was cut in the head capsule to expose the surface of the central brain. To facilitate penetration of the electrodes through the brain sheath, 1% collagenase (C-0130, Sigma, St. Louis, MO) in cricket saline was applied for 1–3 min. Intracellular signals from polarization-sensitive neurons were recorded with electrodes aimed at the central complex. We used quartz micropipettes produced on a laser puller (Model 2000, Sutter Instruments, Novato, CA). The electrode tips were filled with 4% Neurobiotin (Vector Laboratories, Burlingame, CA) in 2 M KCl, and the shanks were filled up with 2 M KCl. DC electrode resistances ranged from 100 to 200 MΩ. The experiments were performed with a conventional setup for intracellular recordings including a high-impedance electrometer (Cyto 721, World Precision Instruments, Sarasota, FL) at the first amplification stage. Neural signals (in AC mode), polarizer orientation and shutter state were displayed on an oscilloscope and recorded with a DAT recorder (DTR 1800, Bio-Logic, Claix, France). Cells were injected with Neurobiotin by applying depolarizing current of 1–3 nA for 1–5 min.

VISUAL STIMULATION. The light of a blue high-power LED (λ_{max} = 450 nm; half-width = 30 nm; LED450-66-60, Roithner Lasertechnik, Vienna, Austria) was focused into a flexible light guide by a glass lens. The light leaving the other end of the light guide illuminated a circular diffusor (2 layers of tracing paper) of 46 mm diam. directly overlying a linear polarizer (HN38, Polaroid, Cambridge, MA) of the same size. Diffusor and polarizer were mounted together in a circular filter holder that could be rotated by a DC motor. The stimulus was centered at the animal's zenith (with respect to natural head position) at a distance of 63 mm from the cricket head, providing a dorsal, polarized stimulus of 40° diameter. Elliptically polarized stimuli were produced by combining the linear polarizer with an optical retarder (Connect overhead projection film, Interaction-Connect, Gent, Belgium). Different ellipticities could be generated by adjusting the axis of the retarder relative to the transmission axis of the polarizer. For theoretical reasons and as demonstrated experimentally, partially plane-polarized light and elliptically polarized light with the same d value (a measure of both the degree of polarization and ellipticity) are equivalent for a photoreceptor cell (for a detailed discussion, see Labhart 1996). Thus for our experiments, three polarized stimuli with different d values were available: $d = 0.99$ (linear polarization), $d = 0.59$, and $d = 0.18$ (elliptical polarization). The exact d value and the prevailing e-vector orientation of each stimulus were measured photometrically (Optometer Model 161 with detector head 222AUV by United Detector Technology, Hawthorne, CA, fitted with a linear polarizer HNP'B by Polaroid). Absolute light intensities were $\sim 3 \times 10^{12}$ photons s^{-1} cm^{-2} (5 neurons) or $\sim 6 \times 10^{12}$ photons s^{-1} cm^{-2} (45 neurons). In a few experiments (5 neurons) at the beginning of the study, the polarizer was positioned closer (35 mm) to the cricket head providing a dorsal stimulus of 67° diameter and $d = 0.99$ at a light intensity of 1.3×10^{13} photons s^{-1} cm^{-2}. Sometimes the stimulus was depolarized by inserting a diffusor between the polarizer and the insect. This reduced light intensity by ~0.2 log units. All light intensities were >4 orders of magnitude above the absolute threshold of cricket polarization vision; see Herzmann and Labhart 1989). Behavioral experiments (Herzmann and Labhart 1989) and electrophysiological recordings from POL1 neurons (Labhart and Petzold 1993) indicate that the e-vector detection system is insensitive to light intensity (above the absolute threshold), suggesting that slight intensity changes do not influence the response of central polarization-sensitive neurons. To measure the e-vector response of the neurons, the eyes were stimulated with continuous light with the prevailing e-vector rotating at a constant angular velocity of ~60° s^{-1}.

EXPERIMENTAL PROTOCOL. To obtain intracellular recordings from polarization-sensitive neurons, the electrode was aimed at the central complex and advanced in small steps into the brain while the eye was stimulated by polarized light with rotating e-vector. Once a polarization-sensitive cell was penetrated, which was clearly indicated by the modulating spike frequency, the response to two or three 360° clockwise rotations of e-vector orientation followed by the same number of anticlockwise rotations was recorded. Then the shutter was closed for ~10 s to record the dark activity of the cell and sometimes the response to unpolarized light was recorded.

EVALUATION OF DATA. The DAT recorded original data were transferred to a computer and evaluated with a custom made program written in IGOR Pro (Wavemetrics, Lake Oswego, OR). We obtained e-vector response functions by counting the number of action potentials in 20° bins of e-vector orientation (corresponding to 0.33 s), with either 5° spacing of the bins (15° overlap) or 20° spacing (no overlap). Mean e-vector response functions were calculated by averaging the spike counts of corresponding bins of all clockwise (cw) and all counterclockwise (ccw) 360° rotations of each neuron. We used these functions to determine the e-vector orientation eliciting maximal spike frequency φ_{max}, which we defined as the e-vector for which the areas under a given activity peak on both sides of φ_{max} were equal. The mean cw and ccw φ_{max} values were averaged to obtain each neuron's specific e-vector tuning axis φ_{max}. The modulation amplitude of the e-vector response was defined as the difference between the average maximal and minimal spike frequencies in the averaged cw e-vector response function of each neuron. In this study, e-vector orientations are always indicated relative to the long axis of the head (clockwise and as seen from above).

HISTOLOGY OF INTRACELLULAR DYE MARKINGS. After recording and dye injection, the cricket head was immersed in fixative for 1 h, and then the brain including the optic lobe was dissected out of the head capsule. The preparation was fixed for 3 h at room temperature or overnight at 4°C in 4% paraformaldehyde, 0.25% glutaraldehyde, and 0.2% saturated picric acid in 0.1 M phosphate buffer (PB, pH 7.4). After rinsing in PB for ≥12 h, the brain was immersed in 70% ethanol for 30 min to block endogenous peroxidase activity. After rinsing in PB, the brain was incubated for 40 h at 4°C with ABC (Vectastain Elite ABC Kit, Vector Laboratories, Burlingame, CA) made up in PB with 0.1% Tween (TPB). After rinsing in PB, the brain was subsequently incubated for 1h at 4°C in the dark with a solution of 0.07% 3,3′-diaminobenzidine tetrahydrochloride and 0.02% $NiCl_2$ in TPB. To prevent staining on the surface, the brain was dipped into TPB once and then treated with 0.03% H_2O_2 in TPB for 5–10 min. Then the brain was rinsed in PB several times, dehydrated through an ethanol series and cleared in methyl salicylate. All neurons were traced in whole-mount preparations using a Zeiss microscope (Axiophot) with a drawing tube attachment.

RESULTS

Neural network model: original version

GENERAL PROPERTIES. The neural network model (Fig. 1*A*) attempts to explain in which way the signals of three e-vector types of POL neuron, such as found in the insect optic lobe, could be converted to the activity of specific "compass neurons" by using simple neural operations (see METHODS). To assess the performance of the model, we used simulated input, i.e., the e-vector responses of the input neurons (model POL neurons) follow log $\cos^2$ functions (see METHODS; Fig. 1*B*, *top graph*). By using a noise-free environment, we evaluated the potential performance of the model, i.e., we tested for systematic errors (nonlinearities) and excluded the influence of signal noise on coding precision from our considerations (see DISCUSSION). For each e-vector orientation, the neural network receives a signal from each of the three model POL

neurons (signal triplet) and produces a distinct activity pattern in the third layer of neurons (compass neurons) in the form of a group of active neurons. Figure 1, *B* (*top graph*) and *C,* depicts the POL neuron signals and the activity patterns among the compass neurons for a number of e-vector orientations. For instance, at an e-vector orientation of 90°, the activity pattern is centered on compass neuron number 7 (representing 90°; Fig. 1*C*, *top graph*). Rotating the e-vector by 15° results in a shift of the activity pattern by one neuron with the center on neuron 8 (Fig. 1*C*, *middle graph*). As seen by consulting Fig. 1*B* (*bottom graph*), this behavior is consistent, i.e., the activity pattern always shifts as the e-vector orientation changes. A rotation of the e-vector by 180° leads to a complete rotation of the activity pattern along the neural array as if the two ends of the array were connected to form a ring.

The activity patterns have distinct features. First, the active neurons always form one cluster, i.e., simultaneously active neurons represent similar preferred e-vectors. Second, the neurons in the center of the cluster are more active than those in the periphery. And third, the cluster shifts consistently to the right or to the left as the e-vector rotates clockwise or anticlockwise, respectively, i.e., it behaves like the needle of a compass. Thus the neural network converts the signal triplet provided by the model POL neurons into a spatial representation of e-vector orientation in the form of a specific population of active output neurons. Although there is a finite number of compass neurons, population coding allows a high precision of e-vector coding. This is because encoding is not discrete, i.e., orientation is not indicated by single neurons but rather by a group of neurons with overlapping e-vector response functions (compare Georgopoulos et al. 1988; Lee et al. 1988, for coding motion in motor cortex; McNaughton et al. 1996; for coding head direction in dorsal presubiculum).

INDICATION OF E-VECTOR ORIENTATION BY COMPASS NEURONS AT DIFFERENT DEGREES OF POLARIZATION. In a polarization compass, the relation between actual e-vector orientation and indicated orientation should be linear. The algorithm presented by Lambrinos et al. (2000) and successfully used in a navigating robot (Lambrinos et al. 2000) provides this linearity; it is the mathematical solution to the problem of extracting e-vector orientation from the signals of three model POL neurons with log $\cos^2$ e-vector response functions. In addition, a useful polarization compass should be insensitive to the degree of polarization *d*. This is because the degree of polarization experienced by the insect POL neurons varies strongly depending on sky conditions (low vs. high solar elevation, clear vs. cloudy sky) (see Labhart 1999). In the network model, the activation pattern of the compass neurons (Fig. 1*C*) represents the output of the polarization compass, providing the insect with a map-like representation of e-vector orientation. To assess the precision of that map, i.e., the linearity of the model, we used the population median of the active compass neurons as a measure (see METHODS) and compared it with the actual e-vector orientation (Fig. 2).

For degrees of polarization $d \leq 0.55$, the orientations indicated by the population medians are very close to the actual orientation (differences $<0.3°$) and virtually independent of *d* (Fig. 2*A*). For practical purposes, such minute errors can be neglected. The observed small nonlinearities of the network model are effects of the mathematical algorithm used to calculate the population median and not an intrinsic property of population coding. Errors occur because the threshold operation removes information at the network output. For $d \leq 0.52$, the errors follow a sinusoidal function with a period of 15° (Fig. 2*A*).

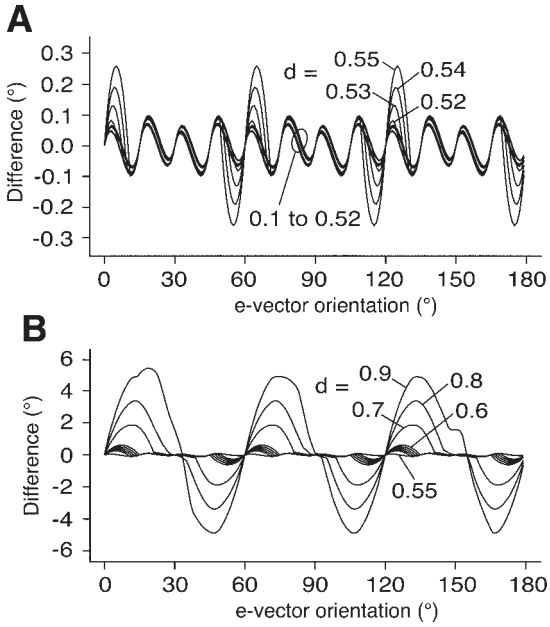

FIG. 2. Performance of the neural network model indicated by the differences between the population median of the compass neurons and the actual e-vector orientation (errors). Numbers in graphs indicate degrees of polarization *d*. *A*: error functions for $d = 0.1–0.55$. *B*: error functions for $d = 0.55–0.9$. The differences are identical for the original and the extended network model. Note that for physiological degrees of polarization ($d \leq 0.55$), the errors are $<0.3°$.

At physiologically unrealistic degrees of polarization ($d > 0.55$; compare DISCUSSION), the model becomes increasingly nonlinear, and for $d = 0.9$, the errors can reach ~5° (Fig. 2*B*). This is because the modulation amplitude of the e-vector response functions of the input neurons (model POL neurons) increases such that near the e-vector of minimal excitation the spike frequency drops to zero and the sinusoidal shape of the response functions becomes clipped. This simulates the behavior of actual POL1 neurons (Labhart 1996).

ACTIVITY LEVELS OF COMPASS NEURONS AT DIFFERENT DEGREES OF POLARIZATION. Figure 3, *A* and *B,* exemplifies the e-vector response functions of the model POL neurons (*A*) and the activity patterns of the compass neurons for an e-vector orientation of 105° (*B*) at two degrees of polarization ($d = 0.4$ and $d = 0.2$). Although shape and position of the activity patterns are the same, the activity levels of the active compass neurons clearly change with *d*. As shown in Fig. 3*E* for three representative e-vector orientations, compass neuron activity (summed activity of all active neurons) steadily increases with increasing *d*. The basis for this correlation is that the modulation amplitudes of the model POL neuron responses are functions of *d* (Fig. 3*D*), again simulating insect POL1 neurons (Labhart 1996).

In conclusion, the neural network model converts the signals of three model POL neurons to a specific population of active compass neurons. Although the output activity of the network

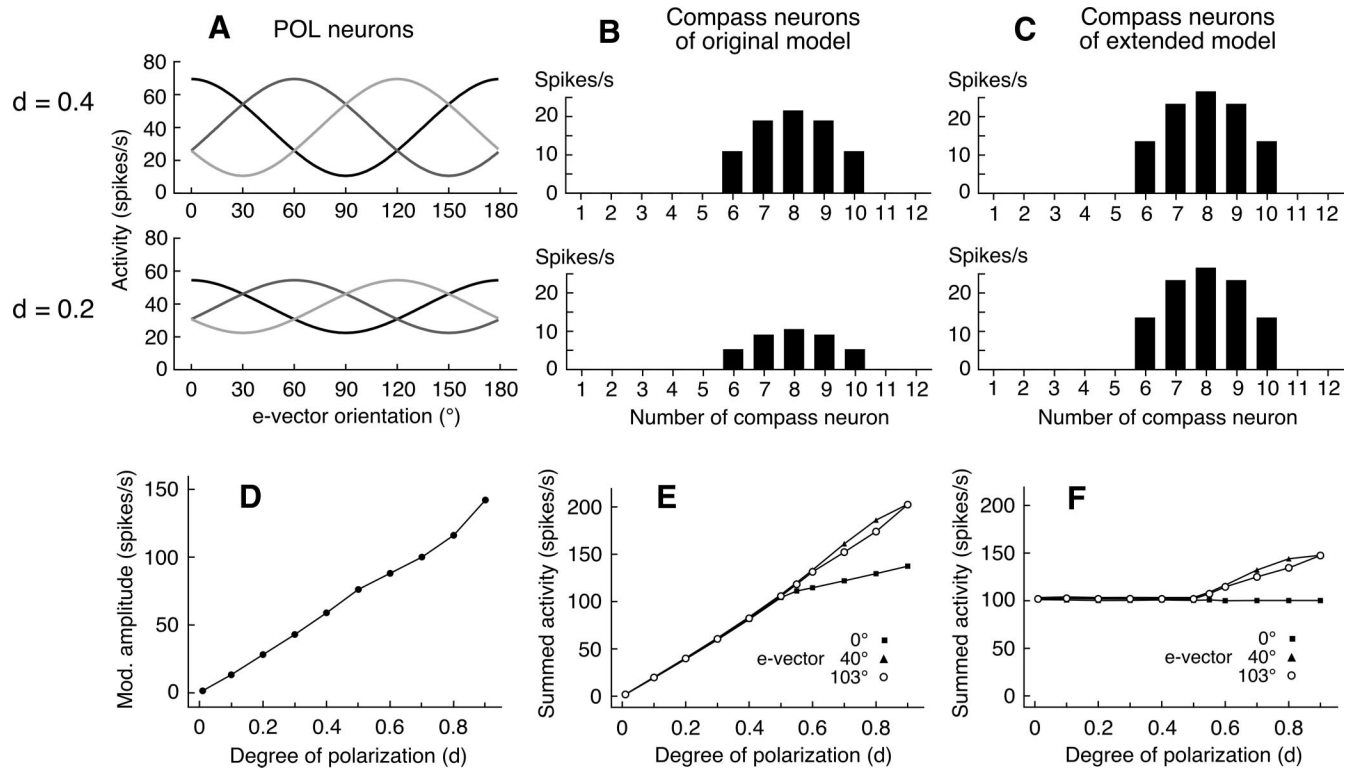

FIG. 3. Activity levels of model POL neurons and compass neurons at different degrees of polarization *d*. *A*: e-vector response functions of POL neurons. *B* and *C*: activity patterns of compass neurons with the original (*B*) and the extended network model (*C*) for $d = 0.4$ and $d = 0.2$ (*top* and *bottom,* respectively). *D*: modulation amplitudes of POL neuron activities as a function of *d*. *E* and *F*: sum of compass neuron activities for the original (*E*) and the extended network model (*F*) as a function of *d* at 3 representative e-vector orientations.

varies as a function of the degree of polarization *d*, the population median of active compass neurons remains practically constant and indicates e-vector orientation with high precision as long as *d* remains in the physiological range.

Electrophysiological recordings

GENERAL PROPERTIES OF THE POLARIZATION-SENSITIVE NEURONS. The neural network model proposes a plausible way for coding e-vector orientation in a nervous system at the output of a polarization compass. To test if neurons with the response profile of compass neurons actually exist in the cricket brain, we set out to study the physiology and the morphology of neurons in an area of the insect brain that is believed to be a center for spatial orientation (Homberg 2004; Vitzthum et al. 2002). We recorded from 55 polarization-sensitive neurons in the central complex of the cricket brain. In these neurons, spike rate was a periodic function of e-vector orientation with a period of 180°, i.e., there were two activity maxima per 360° e-vector rotation. In most neurons, the activity maxima were separated by e-vector ranges, in which the neurons remained silent or showed only very low spike activity (Figs. 4 and 5). Some neurons had asymmetrical response peaks (Fig. 6*B*). The direction of asymmetry was always independent of the direction of stimulus rotation (clockwise or anti-clockwise). Apparently these neurons received somewhat asymmetrical input from lower order neurons. The responses to the slowly rotating e-vector were typically vigorous for both strong and weak polarization: maximal spike rates at the e-vector of maximal activity φ_{max} were 19.7 ± 9.4 spike/s (average ± SD), and the modulation of spike rate (difference between maximum and minimum activity) was 16.9 ± 9.0 spike/s. Twenty-six of the 55 neurons were successfully injected with Neurobiotin and could be studied morphologically. Based on their response properties, we distinguished between three categories of polarization sensitive neurons.

COMPASS NEURON-LIKE CELLS I. Twenty neurons showed no activity in the dark and between the response maxima. (Fig. 4*A*, see Polarized light and Dark; Fig. 8, *B* and *C*). The maximal spike frequency (at φ_{max}) varied from 8.5 to 39 spike/s between individual neurons. When the rotating e-vector was stopped at φ_{max}, the neurons continued firing tonically. Two preparations were also stimulated with unpolarized light, which produced only a few irregular spikes (Fig. 4*A*, Unpolarized light) with average spike frequencies of 1.2 and 0.7 spike/s, respectively. We call this category of neurons "compass neuron-like cells I" (CNL I) because it exhibits the same characteristics as the modeled compass neurons (Fig. 1*B*, *bottom graph*), i.e., the response maxima are separated by silent e-vector ranges (Figs. 4, *A* and *B,* and 8, *B* and *C*). We stained 11 of these 20 neurons by Neurobiotin. All neurons showed similar morphological properties (Fig. 4*C*), and they strongly resembled the tangential neurons in the locust central complex (Müller et al. 1997). The cell body was located in the inferio-median protocerebrum, close to the antennal lobe. A neurite ran into the lateral accessory lobe (LAL) where it had several collaterals and arborizations. Seven of the stained neurons showed branching in the lateral part of the LAL only (Fig. 4*C*, *middle neuron*). Four neurons formed collaterals and

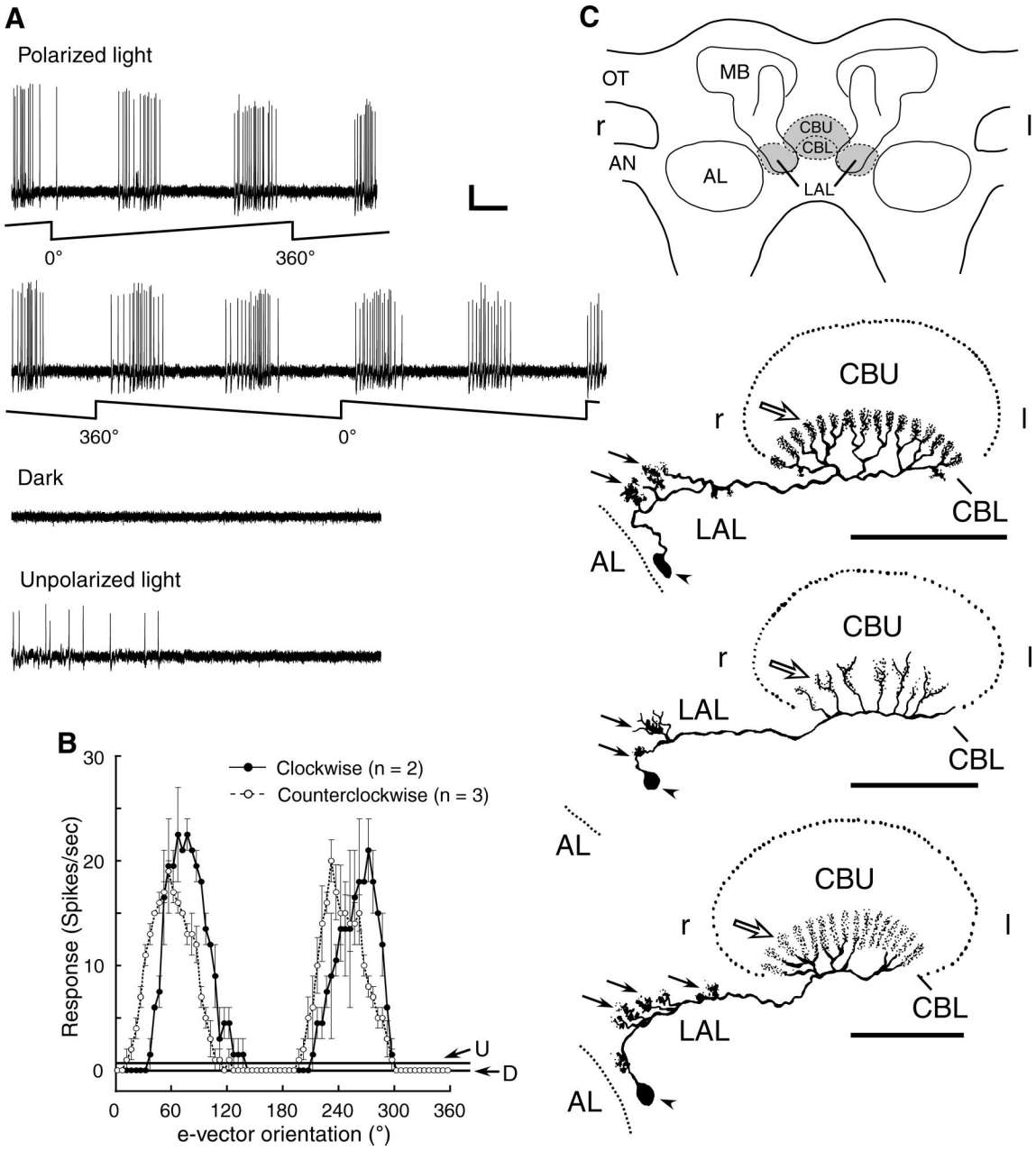

FIG. 4. Polarization-sensitive neurons with no spontaneous activity [compass neuron-like (CNL) I, see text]. *A*: traces of an intracellular recording. *Top two recordings* (Polarized light) show responses to slowly rotating e-vector orientation (degree of polarization $d = 0.18$). Sawtooth-shaped traces below neural signals indicate e-vector orientation rotating in clockwise (top recording, rising ramps) and counterclockwise direction (bottom recording, falling ramps). *Lower two recordings* show activities in the dark (Dark) and with unpolarized light (Unpolarized light). Calibration: 10 mV, 1 s. *B*: averaged e-vector response functions for clockwise and counterclockwise e-vector rotation. *X* axis indicates e-vector orientation relative to the long axis of the head (clockwise and as seen from dorsal). D and U give average spike rates in the dark and with unpolarized light, respectively. Symbols: average spike counts per 20° bin of e-vector rotation taken at 5° intervals; error bars: SE; *n,* number of 360° polarizer rotations. *C*: morphology of 3 CNL I cells. Electrophysiological data (*A* and *B*) are from the top neuron. The neurons have their cell bodies (arrowheads) in the inferio-median protocerebrum and arborize in the lateral accessory lobe (LAL; black arrows) and in the lower part of the central body (CBL; empty arrow). AL, antennal lobe; AN, antennal nerve; CBU, upper part of central body; OT, optic tract; r, right; l, left. Scale bars: 100 μm.

arborizations along the neurite throughout the LAL (Fig. 4*C*, *top* and *bottom neuron*). From the LAL, the neurite ran through the isthmus tract (Homberg 1987, 1991) to the lower part of the central body (CBL), where it branched off into the CBL (Fig. 4*C*). In some preparations the neuron could be seen to end in 16 distinct columnar ramifications in the CBL (Fig. 4*C*, *top* and *bottom neuron*), in other preparations only the thicker branches were visible (Fig. 4*C*, *middle neuron*).

COMPASS NEURON-LIKE CELLS II. Eighteen neurons had a very low spike frequency in the dark and/or between the response maxima. They exhibited strong excitation and some inhibition (compared with dark activity) under polarized light, but the spike rate often fluctuated especially between the response maxima and in the dark, which was possibly caused by an instability of the recording (Fig. 5*A*). Because of these fluctuations, both the minima of the averaged response functions and

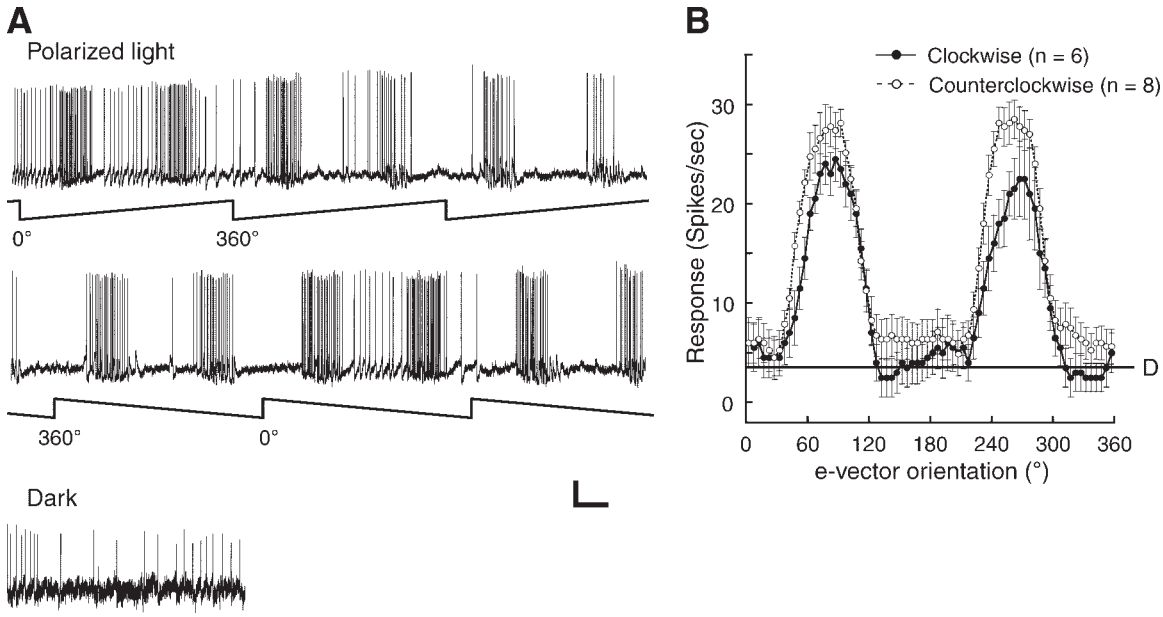

FIG. 5. Polarization-sensitive neuron with low spontaneous activity (CNL II, see text). *A*: traces of intracellular recording. *Top two recordings* (Polarized light) show responses to slowly rotating e-vector orientation (degree of polarization $d = 0.99$). Sawtooth-shaped traces below neural signals and *x*-axis definition are as in as in Fig. 4. Calibration: 10 mV, 1 s. *Bottom recording* shows the activity in the dark (Dark). Calibration: 5 mV, 1 s. *B*: averaged e-vector response functions for clockwise and counterclockwise e-vector rotation. D gives average spike rate in the dark. Symbols: average spike counts per 20° bin of e-vector rotation taken at 5° intervals; error bars: SE; *n,* number of 360° polarizer rotations.

the average activity in the dark where >0 spike/s (Fig. 5*B*), but in between, these neurons behaved like CNL I cells. Spontaneous activities in the dark varied from 0 to 3.8 spike/s, and at the response maximum, spike frequencies ranged from 7.5 to 48 spike/s between neurons. Although these neurons seem to have basically the same response properties as CNL I cells, we created a separate category for them ("compass neuron-like cells II," CNL II) for statistical reasons (see following text). Nine of these neurons were stained with Neurobiotin. They exhibited the same morphology as CNL I cells. Most neurons had the cell body in the same position as the CNL I cells, i.e., in the inferio-median protocerebrum, except for two neurons where the cell body occupied a more lateral position within the inferio-lateral protocerebrum. Five neurons had collaterals and arborizations in the lateral part of the LAL only; the other three neurons branched throughout the LAL. In one of these neurons the characteristic columnar ramifications in the CBL were observed.

PHYSIOLOGICALLY UNCLASSIFIED POLARIZATION-SENSITIVE NEURONS. Seventeen of the 55 polarization-sensitive neurons recorded did not fulfill the criteria for the CNL I or CNL II categories. They include neurons with relatively high spiking activity between the response maxima (range: 4.5–13.5 spike/s; Fig. 6*A*, polarized light) and/or with high activity in the dark (range: 4.0–16.8 spike/s; Fig. 6*A*, Dark) and/or with irregular e-vector response curves. Typically these neurons showed polarization opponency, i.e., strong excitation near the preferred e-vector φ_{max} and weak inhibition at φ_{min} (i.e., $\varphi_{max}+90°$; Fig. 6*B*). Several neurons exhibited a comparatively weak modulation of spike rate only. We stained six of these neurons by Neurobiotin. They exhibited the same morphology as the neurons in categories CNL I and CNL II. The cell body was located in the inferio-median protocerebrum and the neurite had several collaterals and arborizations, mostly in the lateral part of the LAL (Fig. 6*C*). In two preparations, the columnar structure of the ramifications in the CBL was clearly visible (Fig. 6*C*).

STATISTICAL GROUPS OF DATA. For statistical analysis, we defined three groups of data. The first group ("CNL I") contains the data from CNL I cells only, i.e., from those cells that behaved like compass neurons by the most strict criteria (no activity in the dark and between response maxima). The second group ("CNL I + CNL II") combines the data from CNL I cells with those of CNL II cells, neurons that fulfill the criteria for compass neurons by somewhat less strict criteria (low spike activity in the dark and between maxima allowed). The third group ("All Neurons") includes the data of all 55 polarization-sensitive neurons recorded irrespective of their response properties. As argued in DISCUSSION, both the statistical analysis and the morphological data suggest that all three response categories of neurons (CNL I, CNL II, unclassified) represent the same type of neuron.

DISTRIBUTION OF E-VECTOR TUNING AXES (φ_{max}). In a number of neurons, there was a slight difference of 10–20° between the preferred e-vector φ_{max} obtained with clockwise (cw) and counterclockwise (ccw) e-vector rotation. In most cases, this divergence can be explained by a response delay, i.e., $\varphi_{max,cw}$ had a higher angular value than $\varphi_{max,ccw}$ (Fig. 4*B*). However, in a few cells, the opposite divergence occurred. This could be caused by an adaptation effect such that a neuron, while climbing an e-vector response peak, constantly loses some of its responsiveness. In 60% of the neurons, the difference between $\varphi_{max,cw}$ and $\varphi_{max,ccw}$ was <10°.

The e-vector tuning axes φ_{max} were calculated for each polarization-sensitive neuron by averaging the φ_{max}values obtained with clockwise and anti-clockwise stimulation to neutralize a possible bias induced by the constantly rotating e-vector. Neurons in which maximal activity was not clearly

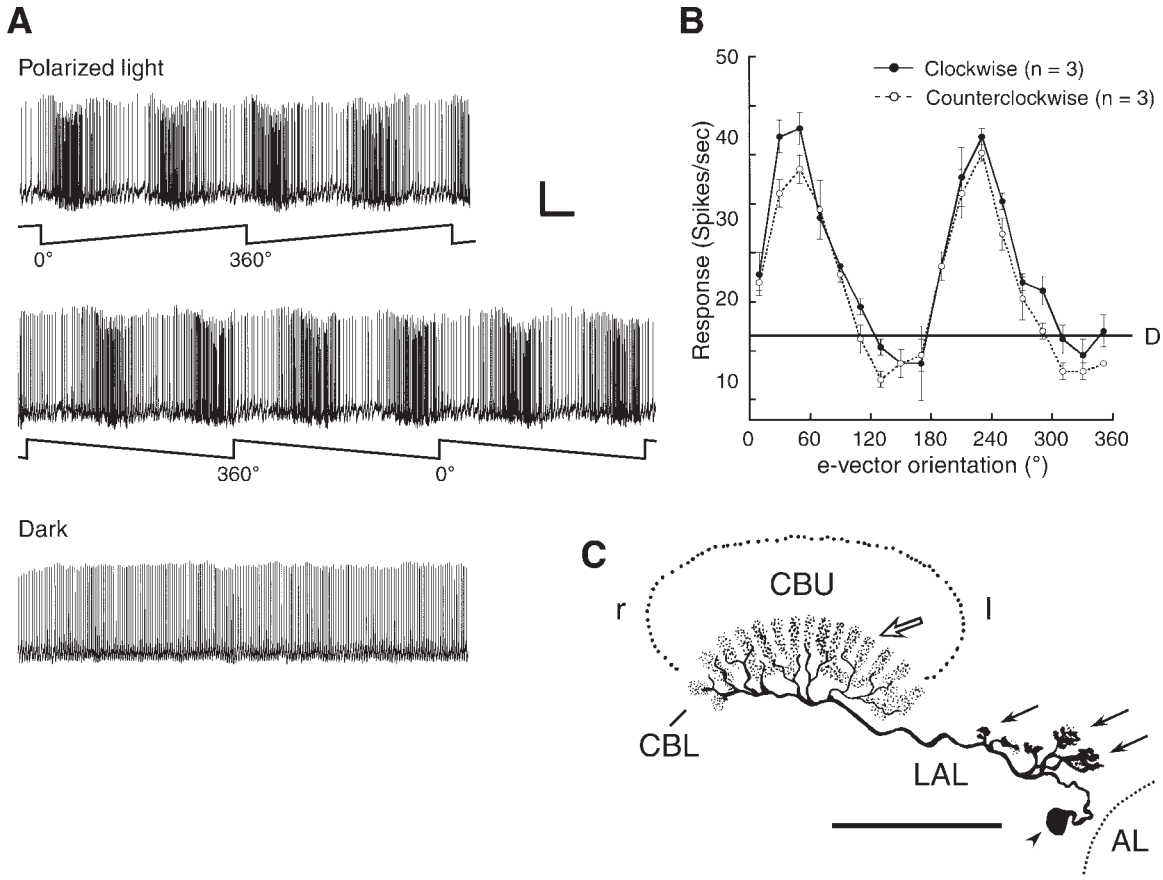

FIG. 6. Polarization-sensitive neuron with high spontaneous activity (physiologically "unclassified" type, see text). *A*: traces of an intracellular recording. *Top two recordings* (Polarized light) show responses to slowly rotating e-vector orientation (degree of polarization $d = 0.99$). Sawtooth-shaped traces below neural signals and *x*-axis definition are as in Fig. 4. *Bottom recording* gives activity in the dark (Dark). Calibration: 10 mV, 1 s. *B*: averaged e-vector response functions for clockwise and counterclockwise e-vector rotation. D gives average spike rates in the dark. Symbols: average spike counts per 20° bin of e-vector rotation taken at 20° intervals; error bars: SE; *n,* number of 360° polarizer rotations. *C*: morphology of neuron. The neuron has its cell body (arrowhead) in the inferio-median protocerebrum and arborizes (arrows) in the LAL and in the CBL (empty arrow). Scale bar: 100 μm.

defined (noisy or very wide response maxima) were excluded from this evaluation. Figure 7*A* shows the φ_{max} distribution of the three data groups. In all statistical groups, the φ_{max} values cannot be ascribed to particular e-vector types, but they are randomly distributed between 0 and 180° (CNL I, $P > 0.05$; CNL II, $P > 0.1$; CNL I + CNL II, $P > 0.5$; all neurons, $P > 0.5$; Rao's spacing test). The distributions of the φ_{max} values for the different data groups do not differ statistically among each other ($P > 0.5$, Watson's *U* test). For the marked cells alone, the φ_{max} values are also randomly distributed ($P > 0.1$, Rao's spacing test) in all statistical groups. No correlation could be made between e-vector tuning axes φ_{max} and any morphological feature visible in the whole-mount preparations (compare Heinze and Homberg 2007).

Because of the westward movement of the sun, the readings of both sun and polarization compass must be time-compensated to be useful for orientation relative to geographic directions. Therefore individual compass neurons might change their e-vector tuning axes in the course of the day. Because the recordings were done at different times of the day (usually between 4 p.m. and 8:30 p.m.), the presence of just a few e-vector types of neurons (as in the case of the POL1 neurons) could be masked. However, if the φ_{max} values are graphed versus time of the day, the values appear randomly distributed and there are no evident clusters (data not shown). In principle, the φ_{max} values could be time-compensated before graphing them as histograms (compare e.g., Stalleicken et al. 2005). However, the crickets were raised and kept under artificial, long-day lighting, and it is unknown after which rule their navigation system is time-compensated if there is time compensation at all under these conditions.

RESPONSE AMPLITUDE AT DIFFERENT DEGREES OF POLARIZATION. We have used three different degrees of polarization *d* for stimulating the neurons. Values of *d* experienced by crickets under natural conditions have been estimated by Labhart (1999) by recording the responses of an opto-electronic simulation of a POL1 neuron to natural skylight polarization. A polarized stimulus with $d = 0.99$ as obtained by a sheet polarizer is much stronger than a cricket will ever experience under the sky. Thus to adapt the stimulus to more natural conditions, we also used stimuli with weaker polarization. A *d* value of 0.59 is close to the highest polarization level a cricket is expected to meet under the optimal conditions of a clear sky with low solar elevation. The stimulus with $d = 0.18$ approximates conditions under partly cloudy skies and/or relatively high solar elevations.

As exemplified in Fig. 8, *A–C,* for one CNL II and two CNL I cells, the neurons respond strongly under all three degrees of polarization (see also Fig. 4, *A* and *B,* with $d = 0.18$, and Fig.

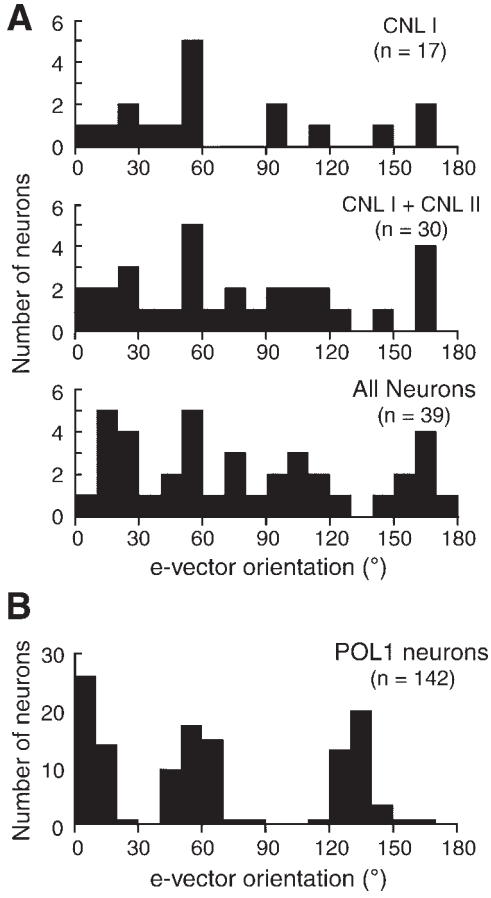

FIG. 7. e-vector orientations (φ_{max}) of zenithal stimuli eliciting maximal spike frequencies in different polarization-sensitive neurons of the cricket visual system. φ_{max} values are defined with respect to the long axis of the head (clockwise and as seen from above). *n,* number of neurons tested. *A*: neurons of the central complex. Data for statistical groups CNL I, CNL I + CNL II and All Neurons (*top* to *bottom graph*). Degree of polarization *d* was 0.99, 0.59, or 0.18. *B*: POL1 neurons in the optic lobe. Degree of polarization *d* was 1.0. (after Labhart and Meyer 2002). Note that there are 3 types of POL1 neuron tuned to different e-vector orientations, whereas central complex neurons are not grouped in particular tuning types and the e-vector tuning axes φ_{max} are randomly distributed ($P > 0.1$ to $P > 0.5$, Rao's spacing test).

5, *A* and *B,* with $d = 0.99$). To compare the strength of the response to the different stimuli, we calculated for each neuron the modulation amplitude of the response, defined as the difference between maximal and minimal spike frequency in the averaged e-vector response function. For this evaluation, we only used the responses to the first two or three (clockwise) rotations of the polarizer because the recording quality was usually better during the first part of the recording and because this way we could include data from cells that were lost after the first few polarizer rotations. The histograms in Fig. 9 show the modulation amplitudes under the three different degrees of polarization for the three statistical groups of neurons. In all groups (Fig. 9, *A–C*), the distributions of modulation amplitudes are similar for the different *d* values (Fig. 9, *top, middle,* and *bottom graphs*) and statistically there is no significant difference for the different degrees of polarization (CNL I, $P > 0.1$; CNL I + CNL II, $P > 0.1$; All Neurons, $P > 0.5$, Kruskal-Wallis test). For the marked cells alone, there is also no relation between response amplitude and *d* ($P > 0.33$, Kruskal-Wallis test), in all statistical groups. This indicates that at least down to $d = 0.18$ the response strength is independent of the degree of polarization. Thus although strongly sensitive to the prevailing e-vector orientation of even weakly polarized skies (compare Labhart 1999), the CNL cells seem to disregard the strength of the polarization signal.

In conclusion, neurons that fulfill the criteria of compass neurons as defined by the network model do indeed exist in the brains of crickets. There is, however, one significant difference: whereas the activity level of the modeled compass neurons varies as a function of *d* (Fig. 3, *B* and *E*), the output level of the actual neurons is constant over a wide range of *d* (Fig. 9).

Neural network model: extended version

To adapt the properties of the model to the electrophysiological findings, we modified the original neural network by adding a fourth layer and by introducing positive and negative feedback loops (Fig. 1*D*). As exemplified in Fig. 3*C* and demonstrated for a wide range of *d* values in Fig. 3*F*, the output activity of the extended network remains constant for $d \leq 0.55$. Only for unphysiologically high *d* values ($d > 0.55$; compare DISCUSSION), activity slightly increases with *d* at certain e-vector orientations. As in the original network, the population median of the active compass neurons indicates e-vector orientation with high precision at physiologically realistic *d* values. The error functions (Fig. 2) for the original and the extended network model are identical. In conclusion, the feedback mechanisms introduced in the extended network model mimic the independence from *d* of CNL cell responses while maintaining the precision of e-vector coding.

DISCUSSION

Neural network model

NEURAL NETWORK ARCHITECTURE. The neural network model is a hypothesis of how the insect brain processes the signals from three polarization-sensitive input channels (triplet code) to form a compass-like neural representation analogous to the head direction cells observed in other animals (population code). The network model is based on an algorithm that differs from the algorithms previously used in navigating robots (Lambrinos et al. 1997, 2000) in the following ways.

First, it uses only simple operations, i.e., addition and subtraction, simulating synaptic excitation and inhibition, respectively, and a threshold function. The robot algorithms contain more complex mathematical elements (e.g., trigonometric functions, look-up tables), which are not readily implemented neurally.

Second, as a result of using only simple mathematical operators, our model provides a parsimonious solution, which can readily be represented as an artificial neural network containing a comparatively small number of neural elements. It could be implemented both electronically and neurally as a simple analog circuit. In comparison, the implementation of one trigonometric function alone would already involve a certain number of neurons, increasing both the number of elements and the complexity of a network.

Third, the output is compatible with a population code for representing e-vector orientation in the brain. In actual brains, visual features such as edge orientation (e.g., Bonhoeffer and Grinwald 1993; Hubel and Wiesel 1968), movement direction

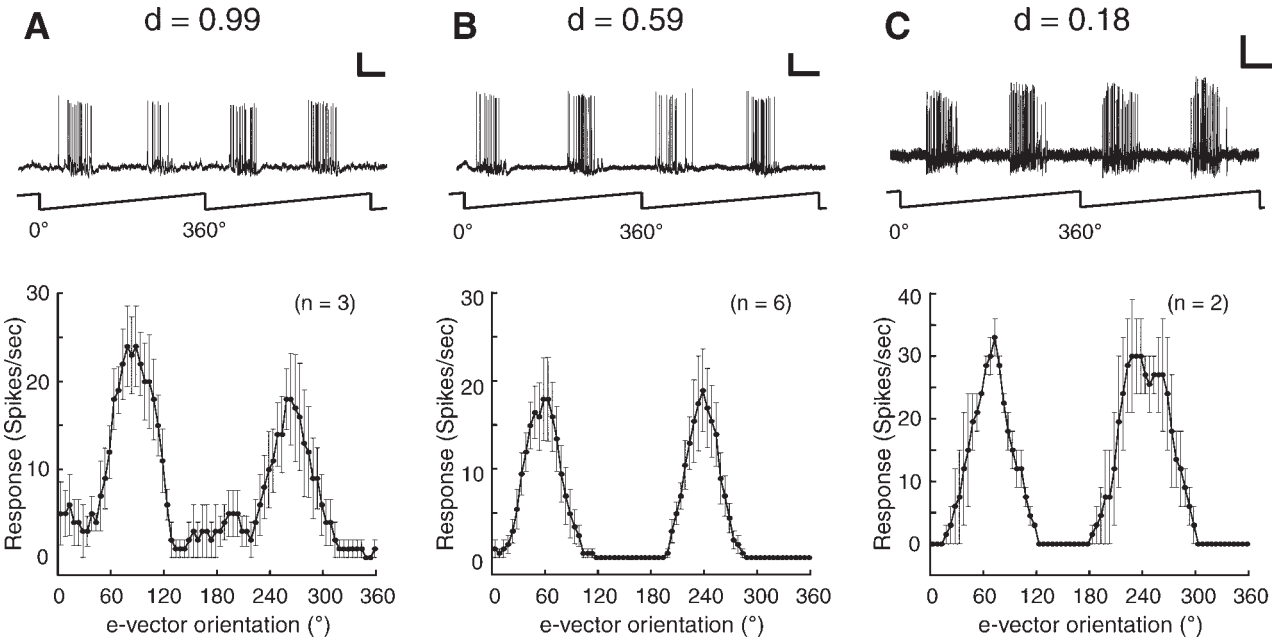

FIG. 8. e-vector responses of CNL cells at different degrees of polarization. Responses of a CNL II cell (*A*) and 2 CNL I cells (*B* and *C*) to slow clockwise rotation of e-vector orientation with different degrees of polarization ($d = 0.99$, 0.59, and 0.18, respectively). Traces of intracellular recordings (*top graphs*) and e-vector response functions (*bottom graphs*). Sawtooth-shaped traces below neural signals and *x*-axis definition are as in Fig. 4. Error bars, SE; *n,* number of 360° polarizer rotations. Calibration: 10 mV, 1 s. Note that crisp e-vector responses can be elicited with both strongly and weakly polarized stimuli.

(e.g., Wellky et al. 1996), spatial frequency (e.g., Tootell et al. 1988), and color (e.g., Ts'o and Gilbert 1988; Xiao et al. 2003) are population coded (position coded), i.e., they are indicated by the position of a group of active neurons in the relevant brain areas. The same is true for the coding of head orientation relative to a visual environment (Taube 1998). By assigning an activity level to each of the differently tuned compass neurons, the output of the network model provides this population code. In contrast, at the output of the robot algorithms e-vector orientation is represented by just one number. Neurally this could be expressed by an activity code where the spike frequency of a single neuron codes e-vector orientation. In the visual system no cases of activity coding are known.

These properties make our model more compatible with natural e-vector coding systems than the purely mathematical solutions used for robot navigation (Lambrinos et al. 1997, 2000). However, by simply adding and subtracting spike frequencies, the synaptic connections of the network are gross simplifications of real synapses that are only acceptable under certain constraints: *1*) linear conversion of input spike frequency to postsynaptic potential, *2*) linear interaction between

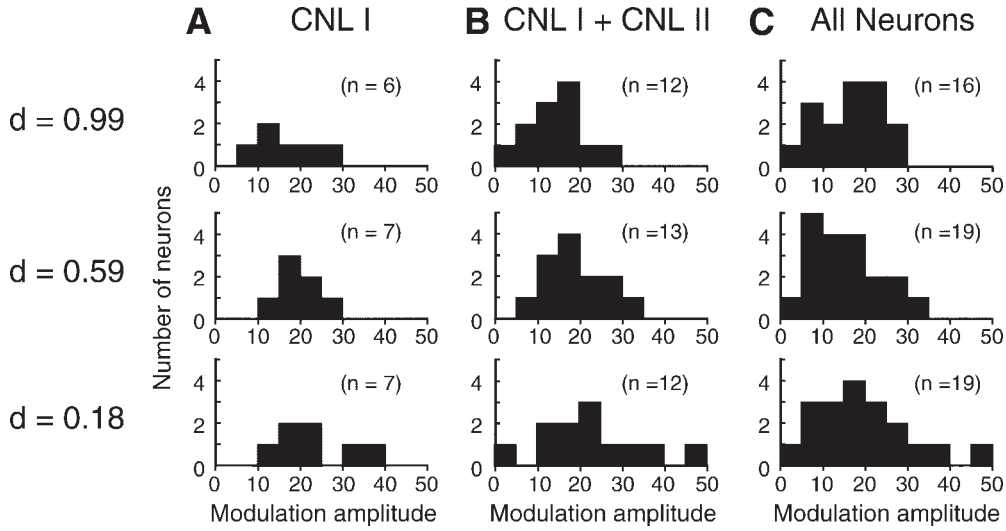

FIG. 9. Strength of the e-vector response at different degrees of polarization *d*. Histograms give the modulation amplitude of the e-vector response under different degrees of polarization ($d = 0.99$, 0.59, and 0.18, corresponding to top, middle, and bottom lines of graphs, respectively) for the three statistical groups of neurons (CNL I, CNL I + CNL II, and All Neurons, corresponding to columns *A–C*). Modulation amplitude is defined as the difference between maximal and minimal spike frequency of the averaged e-vector response function. In all groups (*A–C*), the distributions of modulation amplitudes do not differ statistically for different degrees of polarization (CNL I, $P > 0.1$; CNL + CNL II, $P > 0.1$; all neurons, $P > 0.5$, Kruskal-Wallis test). *n*, number of neurons. Note that the strength of the e-vector response is independent of the degree of polarization.

postsynaptic potentials from different synapses resulting in a generator potential, and *3*) linear conversion of generator potential to output spike frequency. To provide the digital to analog conversion (action potentials to quasi-DC postsynaptic potential) under (*1*), the synapses must have long, integrating time constants, i.e., the system must have a long shutter time. Processing by parallel, independent networks could further reduce noise in the system.

While input and output layers of the (original) neural network are based on physiological data obtained from the cricket visual system (POL1 neurons and CNL cells), neurons with the physiological properties of the intermediate (2nd) layer were demonstrated in the central complex of another orthopteran insect species (locust: Heinze and Homberg 2007; Homberg 2004; Vitzthum et al. 2002). However, it is unknown if the latter neurons actually represent the intermediate layer of the network because the connectivity between the different types of polarization-sensitive neuron in the orthopteran visual system is still unclear. In addition, the mechanisms behind the celestial compasses of crickets and locusts may differ to some extent (Homberg 2004).

In conclusion, the neural network model includes properties that are to be expected in real e-vector coding neural circuits: it uses standard synaptic operations, represents a parsimonious solution, and the model output is compatible with the concept of population coding. In addition, polarization-sensitive neurons with the properties of the neurons employed in the network model have indeed been observed in the orthopteran visual system. We have, however, employed a strongly simplified synaptic functionality. Thus although the network includes properties of real neural circuits, it remains a coarse model. Nevertheless, it demonstrates that a comparatively simple neural circuit involving a small number of neurons and connections may suffice to process e-vector information provided by the peripheral visual system.

The basic (original) network consists of three layers. Because they use linear combinations of the original input, layers 2 and 3 could, in principle, be fused by combining (multiplying) the two connectivity matrices (see *Eqs. A3* and *A5*). We prefer the three-layer architecture because we find the hierarchical proceeding easier to follow: each neuron in layer 2 and 3 receives antagonistic input from just two neurons of the preceding layer. With only two layers, each neuron of the output layer receives multiple inputs through weighted connections, which are difficult to comprehend and to express graphically. In addition, neurons with the response profiles of 2nd layer neurons actually exist in the insect brain (Heinze and Homberg 2007; Homberg 2004; Vitzthum et al. 2002).

Strictly speaking, the triplet code provided by the three types of model POL neuron is already a population code, which is extended at later stages of processing to a larger set of neurons. In our model, this is done by distributing POL neuron activity to 12 compass neurons by feed-forward antagonistic synaptic activity. A threshold operation restricts activity to 50% of all compass neurons at any e-vector orientation, and for each compass neuron, the activity range is restricted to 90° (twice per 360°). By adding additional layers to the network, the number of compass neurons could be increased (doubled by each additional layer). By raising the threshold level, the number of simultaneously active neurons and their activity ranges could be further restricted (consult Fig. 1*B, bottom graph*). We settled for the present version of network because it suffices to demonstrate the principle of the model. In addition, the threshold value chosen (level of inflection points of the sinusoidal response curves) produces activity ranges in the compass neurons which happen to be comparable to those found in the CNL neurons (see Figs. 4*B*, 5*B*, and 8, *B* and *C*).

There is a large literature on population coding dealing with the effects of noise on coding precision (for reviews, see e.g., Averbeck et al. 2006; Deneve et al. 1999; Knill and Pouget 2004; Pouget et al. 2003). By using a noise-free system, we intentionally excluded aspects of noise in our study. Our goal was to propose a plausible mechanism for triplet-to-population-code transformation. To assess the potential performance (linearity) of the network model, a noise-free environment is perfectly adequate.

PERFORMANCE OF THE NEURAL NETWORK MODEL. For $d \leq 0.55$, the neural network performs extremely well, i.e., the relation between e-vector orientation and the population median of active compass neurons is almost perfectly linear. At d values >0.55 the network becomes increasingly nonlinear. As demonstrated with an opto-electronic model of a POL1 neuron, d values experienced by POL1 neurons rarely exceed 0.5 even under optimal sky conditions (clear sky, low sun) (Labhart 1999). Therefore d values >0.55 are physiologically unrealistic and can be disregarded. Apart from studying the performance of the network model with modeled e-vector response functions for input (log $\cos^2$ functions), we have also used input based on actual skylight polarization and found that the performances of the network model and of the robot algorithm (Lambrinos et al. 2000) were perfectly comparable under these conditions (see supplemental on-line material[1]).

The modulation amplitudes of the e-vector response functions of both model POL neurons and POL1 neurons depend on the degree of polarization d (Fig. 3*D*; Labhart 1996). In the *original network model*, the output activity co-varies with the input amplitude but its directional component (population median) remains constant and, therefore such a compass would be perfectly useful. However, in contrast to our expectations from the original network, the data gained from the CNL cells suggest that the output of the polarization compass ignores d. In the *extended network model*, this behavior is emulated by a gain control circuit keeping compass neuron activity at a certain level. Even for $d = 0.01$, the output is restored to the normal level. However, in a biological neural network, noise becomes an important factor at low d values (say, $d < 0.05$) such that the relation between e-vector orientation and active compass neuron population becomes unreliable. Although the network model includes the option of adding noise to the POL neuron signals, we have not yet studied this aspect systematically. The gain control mechanism described in this study has not been physiologically observed so far, but neural circuits with related properties (positive feedback combined with inhibitory neurons) have been proposed elsewhere (e.g., Dragoi and Sur 2000; Hahnloser et al. 2000) to account for various forms of computations in the neocortex such as gain modulation (Chance et al. 2002; Zhang and Abbott 2000) and stimulus selection (Hahnloser et al. 2000).

[1] The online version of this article contains supplemental data.

Electrophysiology and morphology of polarization-sensitive neurons in the central complex

CELL TYPE AND RESPONSE CATEGORIES. Many neurons responded in ways that are comparable to the head direction (HD) cells of rats (Sharp et al. 2001; Taube et al. 1990) and as expected for compass neurons derived from the network model: they showed high spiking activity around the preferred e-vector orientation (φ_{max}) and remained silent at other orientations. Other neurons were clearly polarization-sensitive but were active at all e-vector orientations and/or in the absence of a polarized stimulus, i.e., in the dark. Do the different response properties observed represent different physiological states of one and the same type of neuron or did we record from different types of neurons?

We were able to study the morphology of about half of the physiologically tested neurons. All these neurons are similar in shape and resemble the tangential neurons described in the central complex of locusts, most strongly their TL2 type (Müller et al. 1997). Although some structural variations were observed, the neurons could not be split into different morphological types. Thus regarding the stained neurons, these findings suggest that the recordings were all from the same type of neuron. Given these statistics, there is a good chance that most if not all of the recordings from unmarked cells were also from this cell type. Supporting this view, the statistics of both the distribution of e-vector tuning axes φ_{max} and of modulation amplitude versus degree of polarization d are the same whether the unmarked cells are included or excluded from the evaluation. In addition, the CNL cells could be converted from one response category to another by injecting current. Thus a CNL I cell could be induced to behave like a CNL II cell by applying a suitable amount of depolarizing current and vice versa for hyperpolarizing current.

Adopting the view that our recordings were from the same cell type, what could be the reason for the different response properties observed? Sixty-nine percent of the neurons (38/55) were classified as compass neuron-like cells (CNL I, CNL II). In 66% of these cells (25/38), background activity remained low and stable during the recording; in the remaining 34%, it increased (9/38) or oscillated (4/38). In many cases, the recording was lost after an increase of background activity. This indicates that increased background activity results from deteriorating recording conditions and suggests that the compass neuron-like behavior represents the physiological state of these neurons.

E-VECTOR TUNING AXES (φ_{max}). For all statistical groups of data (CNL I, CNL I + CNL II, and All Neurons; for marked + unmarked cells, and marked cells alone), no particular e-vector types can be recognized, and the e-vector tuning axes φ_{max} are randomly distributed. This corresponds to the core thesis of this study that the central complex contains a set of e-vector-encoding compass neurons. The random φ_{max} distribution of the CNL cells contrasts with the nonrandom φ_{max} distribution of the POL1 neurons in the optic lobe indicating just three e-vector types (compare Fig. 7, *A* with 7*B*).

RESPONSE AMPLITUDE AT DIFFERENT DEGREES OF POLARIZATION. Interestingly, the modulation amplitudes of the e-vector responses were independent of the degree of polarization d of the stimulus. This contrasts with the POL1 neurons in which the modulation amplitudes clearly vary with d (Labhart 1996). It also disagrees with expectations based on the original version of the network model (Fig. 3*D*). Thus by correcting the activity level for variations of d, CNL cells surpass the modeled compass neurons in performance. However, this property agrees with the results of a behavioral study in which the spontaneous response of crickets to e-vector orientation (Brunner and Labhart 1987) showed little variance for d values between 0.2 and 1.0 (Henze and Labhart 2007).

Although the degree of skylight polarization is highly variable, the e-vector orientations as defined by Rayleigh scattering (Strutt 1871) are amazingly stable, providing directional information even under unfavorable sky conditions (Labhart 1999; Pomozi et al. 2001). Thus a polarization compass should rely on the robust signal of e-vector orientation and disregard the degree of polarization d. However, to read prevailing e-vector orientation in weakly polarized skies, the e-vector detecting system must be sensitive enough. Both recordings from POL1 neurons (Labhart 1996) and behavioral tests (Henze and Labhart 2007) indicate that crickets can indeed perceive prevailing e-vector orientations for d values of 0.05 and 0.07, respectively.

POLARIZATION-SENSITIVE NEURONS IN THE CENTRAL COMPLEX OF LOCUSTS. Recordings from neurons in the central complex of another orthopteran insect, the locust *Schistocerca gregaria*, revealed polarization-sensitivity in several types of tangential (TL1, TL2, TL3, TB1) and columnar neurons (CP1, CP2, CPU1) (Heinze and Homberg 2007; Vitzthum et al. 2002). Although responsive to unpolarized light, TL3 neurons with their typically low background activity and vigorous e-vector response resemble our CNL cells physiologically. In TL2 neurons, the e-vector response varied in strength, whereas TL1, CP1, and CP2 neurons typically showed comparatively shallow modulation amplitudes on a background activity. In CPU1 neurons, modulation was strong but on a high background (Heinze and Homberg 2007; Vitzthum et al. 2002; Homberg, unpublished observations). In these studies, white, strongly polarized small-field stimuli ($d \sim 1.0$, diameter: 2–14°) were used, and the influence of d was not tested. The lumped φ_{max} distribution of polarization-sensitive tangential and columnar neurons of different types was random and no particular e-vector types could be distinguished (Vitzthum et al. 2002). Evaluated separately, in both the TL2 and TL3 neurons (resembling cricket CNL cells morphologically and physiologically, respectively) (Homberg 2004; Vitzthum et al. 2002), and in TB1 and CPU1 neurons (Heinze and Homberg 2007) the φ_{max} distributions seem also to be random.

Thus in the orthopteran central complex there are several types of polarization-sensitive neurons in which random distributions of e-vector tuning axes φ_{max} were observed. In principle, each of these neuron types would qualify for population coding e-vector orientation. However, which ones of these neurons represent the output of the polarization compass providing the insect with an orientation reading by a population code and which ones should be regarded as upstream interneurons processing the signals received by the POL neurons? Neurons with limited activity range must be downstream from those with background activity showing the full sinusoidal modulation of activity. This is because the information missing between the activity peaks (no spiking activity) cannot be retrieved at later stages. Therefore the CNL neurons of crickets

(and possibly the TL3 neurons of locusts) seem to be near the compass output. As an alternative, there may be parallel e-vector maps consisting of several populations of compass neurons, and the different polarization-sensitive neurons described are not necessarily arranged in cascading layers.

Compass-neuron-like cells in crickets versus head direction cells of rats

The polarization vision system of crickets is a nonimaging visual subsystem. The only relevant stimulus is e-vector orientation averaged over a large area in the upper sky (Labhart et al. 2001). Because the system is monochromatic, it disregards the spectral composition of a stimulus (Herzmann and Labhart 1989; Labhart 1988; Labhart et al. 1984); because of its antagonism it neglects absolute light level (Labhart 1988) and as suggested by our study, it ignores the strength of polarization d (Figs. 8 and 9). The polarization sensors are specialized photoreceptors in a dedicated eye region (DRA), the structure and physiology of which is well established (Blum and Labhart 2000; Burghause 1979; Labhart et al. 1984; Nilsson et al. 1987; Ukhanov et al. 1996). The combination of a one-dimensional stimulus (e-vector) with a well-defined sensory apparatus (DRA) makes the polarization vision system of crickets a suitable model for studying sensory signal processing and coding of orientation.

The HD cells of rats have much in common with the CNL cells described here (HD cells: Sharp et al. 2001; Taube 1998; CNL cells: present study). Both are active at specific head orientations relative to a visual stimulus. Both provide position-independent compass information. For both, no distinct orientation classes could be defined, i.e., there exists a set of neurons representing different orientations. Models for both systems assume population coding. However, a major difference between the two systems is the complexity of sensory input. Whereas the polarization compass relies on a single visual cue (e-vector orientation in the dorsal visual field), the HD cell system receives visual, vestibular, and even some olfactory input (Taube 1998). The visual input relies on landmarks requiring an imaging visual system. The vestibular input provides angular velocity signals for head turning. Both inputs result from complex multi-step processing of sensory raw data, the details of which are unknown. Therefore models of HD cell networks took for granted the availability of such already processed sensory data for input (Sharp et al. 2001). In contrast, for cricket polarization vision we have a strong concept how the photoreceptor signals (raw data) are processed to produce the observed response characteristics of the input neurons of the network (POL neurons): each tuning type of POL1 neuron receives input from some 200 DRA ommatidia, and antagonistic action of two sets of photoreceptors with mutually orthogonal microvilli (present in each DRA ommatidium) provides the polarization-opponent e-vector characteristic (Labhart et al. 2001).

APPENDIX: FORMAL DESCRIPTIONS OF NEURAL NETWORK OPERATIONS

Response functions of the first-order neurons

The response functions of the first-order neurons are described by

$$p(\varphi) = w + a \log\left(\frac{1 + d\cos(2 * (\varphi - \varphi_{max}))}{1 - d\cos(2 * (\varphi - \varphi_{max}))}\right) \qquad (A1)$$

where $p(\varphi)$ denotes the activity of the neuron at orientation φ, d is the degree of polarization, and φ_{max} *i*s the e-vector tuning orientation (0, 60, or 120°). w and a are scaling parameters setting signal offset and amplitude, respectively, and translating the normalized output signal to spiking activity (spike/s) in a range observed in cricket POL1 neurons (Labhart 1996). Unless indicated otherwise, $a = 80$ spike/s, $w = 55$ spike/s, and the degree of polarization $d = 0.4$.

Response functions of the second-order neurons

The activity of the second-order neurons is described by

$$s_i(\varphi) = f\left(\sum_{j=1}^{3} A_{ji} p_j(\varphi)\right) \text{ for every } i \text{ in } (1,2 \ldots, 6) \qquad (A2)$$

The equation describes the summation of the weighted inputs $p_j(\varphi)$ from the three first-order neurons, where the weights A_{ji} take the values of 1, −1, or 0, representing an excitatory, inhibitory, or no connection, respectively. $s_i(\varphi)$ is the activity of *i*th second-order neuron, $f(x)$ is the response function [in this case the identity function $f(x) = x$], and $p_j(\varphi)$ is the activity of the *j*th first-order neuron (model POL neuron) at orientation φ. The 3×6 connectivity matrix **A** between the POL neurons and the second-order neurons is defined as follows:

$$A = \begin{pmatrix} 1 & 0 & -1 & -1 & 0 & 1 \\ 0 & 1 & 1 & 0 & -1 & -1 \\ -1 & -1 & 0 & 1 & 1 & 0 \end{pmatrix} \qquad (A3)$$

This connectivity pattern represents all possible combination pairs of the three model POL neurons. a, w, and d are as in *Eq. A1*.

Response functions of the third-order neurons

The activity $t_i(\varphi)$ of the third-order neurons is defined by

$$t_i(\varphi) = f\left(\sum_{j=1}^{6} B_{ji} s_j(\varphi)\right) \text{ for every } i \in [1,12] \qquad (A4)$$

where $f(x)$ is the response function of the third-order neurons, $s_j(\varphi)$ is the activity levels of the *j*th second-order neuron and the 6×12 connectivity matrix **B** between the second- and the third-order neurons is defined as follows:

$$B = \begin{pmatrix} 1 & 0 & 1 & 1 & 0 & -1 & -1 & 0 & 0 & 0 & 0 & 1 \\ 0 & 1 & 0 & 0 & 1 & 1 & 0 & -1 & -1 & 0 & 0 & -1 \\ -1 & -1 & 0 & 0 & 0 & 0 & 1 & 1 & 0 & -1 & -1 & 0 \\ 0 & 0 & 0 & 0 & 0 & 0 & 0 & 0 & 1 & 1 & 0 & 0 \\ 0 & 0 & -1 & 0 & 0 & 0 & 0 & 0 & 0 & 0 & 1 & 0 \\ 0 & 0 & 0 & -1 & -1 & 0 & 0 & 0 & 0 & 0 & 0 & 0 \end{pmatrix} \qquad (A5)$$

This connectivity pattern is only 1 of 15 possible ways to combine the activities of the second-order neurons for producing third-order neurons. To reduce spiking activity of the third-order neurons to e-vector ranges of 90°, a spiking threshold is applied. Thus the response functions $f(x)$ of the third-order neurons become threshold functions, which are defined as follows:

$$f(x) = \begin{cases} x, & x > t \\ 0, & x \leq t \end{cases} \quad (A6)$$

where x is the input activity and $t = 55$ spike/s is the threshold level. a, w, and d as in *Eq. A1*.

Response functions of fourth-order neurons (extended model)

The activity $g_i(\varphi)$ of the fourth layer neurons (i.e., the compass neurons of the extended model) is calculated as follows:

$$g_i(\varphi) = k_1 g_i(\varphi) + f(k_2 t_i(\varphi)) \text{ for every } i \in [1,12] \quad (A7)$$

where $f(x)$ is the activity function of the fourth layer neurons [the identity function $f(x) = x$ in this case], k_1 and k_2 are constants set to 0.9 and 0.1, respectively, and $t_i(\varphi)$ is the activity level of the ith third-order neuron. The formula for calculating the activities of the third-order neurons was then extended as follows:

$$t_i(\varphi) = f\left(\sum_{j=1}^{6} B_{ji} s_j(\varphi) + g_i(\varphi), \text{GCN}(\varphi) \right) \text{ for every } i \in [1,12] \quad (A8)$$

where $s_j(\varphi)$ is the activity level of the jth second-order neuron, GCN(φ) is the activity level of the GCN, and the connectivity matrix **B** between the second- and the third-order neurons is the same as before. The activity function of the third-order neurons $f(x,y)$ is defined as follows:

$$f(x, y) = \begin{cases} 0, & y > 0 \\ x, & y \leq 0 \end{cases} \quad (A9)$$

Thus the activity level of the GCN is used as a gate for the activation of the third-order neurons. The activity level of GCN is calculated as follows:

$$\text{GCN}(\varphi) = f\left(\sum_{j=1}^{12} g_j(\varphi) \right) \quad (A10)$$

where $g_j(\varphi)$ is the activity of the jth fourth layer neuron, and the activity function $f(x)$ of the GCN interneuron is a threshold function (the same as in the compass neurons of the original model). The GCN spiking threshold was set to 100 spike/s. Because the new formulas introduce some recurrent parts, which depend on the activity levels of previous time steps, the activity levels are calculated by looping through the formulas until the activity of the compass neurons becomes stable. For simplicity, the time dimension was omitted from the preceding formulas.

Population median of active compass neurons

The weighted average of neural activity (*population median*) is the center of gravity of the active population of compass neurons and is calculated as follows:

$$m(\varphi) = \frac{\sum_{j=1}^{12} j a_j(\varphi)}{\sum_{j=1}^{12} a_j(\varphi)} \quad (A11)$$

where $m(\varphi)$ is the population median and $a_j(\varphi)$ is the activity of the jth compass neuron. In words, the population median is the weighted sum of the compass neuron indices ranging from [1,12] normalized by dividing it by the sum of their total activity.

Implementation of the simulations

The neural network simulator was implemented using the Java programming language and simulations were run on ordinary PCs and Apple computers. The Java classes used for implementing the network architecture were custom developed, while the visualization elements were based on the ptplot classes from the Berkeley Ptolemy project. The complete package can be provided on request.

ACKNOWLEDGMENTS

Present address of M. Sakura: Laboratory of Neuro-Cybernetics, Research Institute for Electronic Science, Hokkaido University, 060-0812 Sapporo, Japan.

GRANTS

Supported by the Swiss National Science Foundation. MS was supported by a postdoctoral fellowship by JSPS (PIJSA-100965).

DISCLOSURE

M. Sakura was supported by a fellowship of the Roche Foundation.

REFERENCES

Averbeck BB, Latham PE, Pouget A. Neural correlations, population coding and computation. *Nat Rev Neurosci* 7: 358–366, 2006.

Bernard GD, Wehner R. Functional similarities between polarization vision and color vision. *Vision Res* 17: 1019–1028, 1977.

Blum M, Labhart T. Photoreceptor visual fields, ommatidial array, and receptor axon projections in the polarization-sensitive dorsal rim area of the cricket compound eye. *J Comp Physiol [A]* 186: 119–126, 2000.

Bonhoeffer T, Grinvald A. The layout of iso-orientation domains in area 18 of cat visual cortex: optical imaging reveals a pinwheel-like organization. *J Neurosci* 13: 4157–4180, 1993.

Brunner D, Labhart T. Behavioural evidence for polarization vision in crickets. *Physiol Entomol* 12: 1–10, 1987.

Burghause FMHR. Die strukturelle Spezialisierung des dorsalen Augenteils der Grillen (Orthoptera, Grylloidea). *Zool Jahrb Physiol* 83: 502–525, 1979.

Chance FS, Abbott LF, Reyes AD. Gain modulation through background synaptic input. *Neuron* 35: 773–782, 2002.

Deneve S, Latham PE, Pouget A. Reading population codes: a neural implementation of ideal observers. *Nat Neurosci* 2: 740–745, 1999.

Douglas RJ, Koch C, Mahowald M, Martin KAC, Suarez HH. Recurrent excitation in neocortical circuits. *Science* 269: 981–985, 1995.

Dragoi V, Sur M. Dynamic properties of recurrent inhibition in primary visual cortex: contrast and orientation dependence of contextual effects. *J Neurophysiol* 83: 1019–1030, 2000.

Georgopoulos AP, Kettner RE, Schwartz AB. Primate motor cortex and free arm movements to visual targets in three-dimensional space. II. Coding of the direction of movement by a neuronal population. *J Neurosci* 8: 2928–2937, 1988.

Hahnloser RHR, Sarpeshkar R, Mahowald MA, Douglas RJ, Seung HS. Digital selection and analogue amplification coexist in a cortex-inspired silicon circuit. *Nature* 405: 947–951, 2000.

Heinze S, Homberg U. Maplike representation of celestial e-vector orientations in the brain of an insect. *Science* 315: 995–997, 2007.

Henze JM, Labhart T. Haze, clouds and limited sky visibility: polarotactic orientation of crickets under difficult stimulus conditions. *J Exp Biol* 210: 3266–3276, 2007.

Herzmann D, Labhart T. Spectral sensitivity and absolute threshold of polarization vision in crickets: a behavioral study. *J Comp Physiol [A]* 165: 315–319, 1989.

Homberg U. Structure and functions of the central complex in insects. In: *Arthropod Brain: Its Evolution, Development, Structure, and Functions*, edited by Gupta AP. New York: Wiley, 1987, p. 347–367.

Homberg U. Neuroarchitecture of the central complex in the brain of the locust *Schistocerca gregaria* and *S. americana* as revealed by serotonin immunocytochemistry. *J Comp Neurol* 303: 245–254, 1991.

Homberg U. In search of the sky compass in the insect brain. *Naturwissenschaften* 91: 199–208, 2004.

Hubel DH, Wiesel TN. Receptive fields and functional architecture of monkey striate cortex. *J Physiol* 195: 215–243, 1968.

Knill DC, Pouget A. The bayesian brain: the role of uncertainty in neural coding and computation. *Trends Neurosci* 12: 712–719, 2004.

Labhart T. Polarization-opponent interneurons in the insect visual system. *Nature* 331: 435–437, 1988.

Labhart T. How polarization-sensitive interneurones of crickets perform at low degrees of polarization. *J Exp Biol* 199: 1467–1475, 1996.

Labhart T. How polarization-sensitive interneurones of crickets see the polarization pattern of the sky: a field study with an opto-electronic model neurone. *J Exp Biol* 202: 757–770, 1999.

Labhart T. Polarization-sensitive neurons in the optic lobe of the desert ant *Cataglyphis bicolor. Naturwissenschaften* 87: 133–136, 2000.

Labhart T, Hodel B, Valenzuela I. The physiology of the cricket's compound eye with particular reference to the anatomically specialized dorsal rim area. *J Comp Physiol [A]* 155: 289–296, 1984.

Labhart T, Meyer EP. Detectors for polarized skylight in insects: a survey of ommatidial specializations in the dorsal rim area of the compound eye. *Microsc Res Tech* 47: 368–379, 1999.

Labhart T, Meyer EP. Neural mechanisms in insect navigation: polarization compass and odometer. *Curr Opin Neurobiol* 12: 707–714, 2002.

Labhart T, Petzold J. Processing of polarized light information in the visual system of crickets. In: *Sensory Systems of Arthopods*, edited by Wiese K, Gribakin FG, Popov AV, Renninger G. Basel: Birkhäuser Verlag, 1993, p. 158–169.

Labhart T, Petzold J, Helbling H. Spatial integration in polarization-sensitive interneurons of crickets: a survey of evidence, mechanisms and benefits. *J Exp Biol* 204: 2423–2430, 2001.

Lambrinos D, Maris M, Kobayashi H, Labhart T, Pfeifer R, Wehner R. An autonomous agent navigating with a polarized light compass. *Adaptive Behav* 6: 131–161, 1997.

Lambrinos D, Möller R, Labhart T, Pfeifer R, Wehner R. A mobile robot employing insect strategies for navigation. *Robot Auton Syst* 30: 39–64, 2000.

Lee C, Rohrer WH, Sparks DL. Population coding of saccadic eye movements by neurons in the superior colliculus. *Nature* 332: 357–360, 1988.

McNaughton BL, Barnes CA, Gerrard JL, Gothard K, Jung MW, Knierim JJ, Kudrimoti H, Qin HY, Skaggs WE, Suster M, Weaver KL. Deciphering the hippocampal polyglot: the hippocampus as a path integration system. *J Exp Bio*l 199: 173–185, 1996.

Müller M, Homberg U, Kühn A. Neuroarchitecture of the lower division of the central body in the brain of the locust (*Schistocerca gregaria*) *Cell Tissue Res* 288: 159–176, 1997.

Nilsson D, Labhart T, Meyer EP. Photoreceptor design and optical properties affecting polarization sensitivity in ants and crickets. *J Comp Physiol [A]* 161: 645–658, 1987.

Petzold J. *Polarisationsempfindliche Neuronen im Sehsystem der Feldgrille, Gryllus campestris*: *Elektrophysiologie, Anatomie und Modellrechnungen* (PhD thesis). Zurich: University of Zürich, 2001.

Pomozi I, Horváth G, Wehner R. How the clear-sky angle of polarization pattern continues underneath clouds: full-sky measurements and implications for animal orientation. *J Exp Biol* 204: 2933–2942, 2001.

Pouget A, Dayan P, Zemel RS. Interference and computation with population codes. *Annu Rev Neurosci* 26: 381–410, 2003.

Sharp PE, Blair HT, Cho J. The anatomical and computational basis of the rat head direction cell signal. *Trends Neurosci* 24: 289–294, 2001.

Stalleicken J, Mukhida M, Labhart T, Wehner R, Frost B, Mouritsen H. Do monarch butterflies use polarized skylight for migratory orientation? *J Exp Biol* 208: 2399–2048, 2005.

Strutt J. On the light from the sky, its polarization and colour. *Phil Mag* 41: 107–120, 1871.

Taube JS. Head direction cells and the neurophysiological basis for a sense of direction. *Prog Neurobiol* 55: 225–256, 1998.

Taube JS, Muller RU, Ranck JB. Head-direction cells recorded from the postsubiculum in freely moving rats. I. Description and quantitative analysis. *J Neurosci* 10: 420–435, 1990.

Tootell RBH, Silverman MS, Hamilton SL, Switkes E, De Valois RL. Functional anatomy of macaque striate cortex. V. Spatial frequency. *J Neurosci* 8: 1610–1624, 1988.

Ts'o DY, Gilbert CD. The organization of chromatic and spatial interactions in the primate striate cortex. *J Neurosci* 8: 1712–1727, 1988.

Ukhanov KY, Leertouwer HL, Gribakin FG, Stavenga DG. Dioptrics of the facet lenses in the dorsal rim area of the cricket *Gryllus bimaculatus*. *J Comp Physiol [A]* 179: 545–552, 1996.

Vitzthum H, Müller M, Homberg U. Neurons of the central complex of the locust *Schistocerca gregaria* are sensitive to polarized light. *J Neurosci* 22: 1114–1125, 2002.

Wehner R. The ant's celestial compass system: spectral and polarization channels. In: *Orientation and Communication in Arthropods*, edited by Lehrer M. Basel: Birkhäuser Verlag, 1997, p. 145–185.

Wehner R, Labhart T. Polarization vision. In: *Invertebrate Vision*, edited by Warrant EJ, Nilsson D-E. Cambridge, UK: Cambridge Univ. Press, 2006, p. 291–348.

Wellky M, Bosking WH, Fitzpatrick D. A systematic map of direction preference in primary visual cortex. *Nature* 379: 725–728, 1996.

Xiao Y, Wang Y, Felleman DJ. A spatially organized representation of color in macaque cortical area V2. *Nature* 421: 535–539, 2003.

Zhang J, Abbott LF. Gain modulation in recurrent networks. *Neurocomputing* 32–33: 623–628, 2000.